
**Separation Science and Technology**
Publication details, including instructions for authors and subscription information:
http://www.informaworld.com/smpp/title~content=t713708471

# On the Charges on the Pore Walls off Microporous Membranes

A. Hernández[a]; J. A. Ibáñez[b]; L. Martinez-diez[c]; A. F. Tejerina[c]
[a] DEPARTAMENTO DE FISICA APLICADA II FACULTAD DE CIENCIAS, UNTVERSID AD DE VALLADOLID, VALLADOLID, SPAIN [b] DEPARTAMENTO DE FISICA FACULTAD DE CIENCIAS, UNWERSIDAD DE MURCIA, MURCIA, SPAIN [c] DEPARTAMENTO DE FISICA APLICADA II FACULTAD DE CIENCIAS, UNWERSIDAD DE VALLADOLID, VALLADOLID, SPAIN

**To cite this Article** Hernández, A. , Ibáñez, J. A. , Martinez-diez, L. and Tejerina, A. F.(1987) 'On the Charges on the Pore Walls off Microporous Membranes', Separation Science and Technology, 22: 4, 1235 — 1254
**To link to this Article: DOI:** 10.1080/01496398708057177
**URL:** http://dx.doi.org/10.1080/01496398708057177

SEPARATION SCIENCE AND TECHNOLOGY, 22(4), pp. 1235-1254, 1987

# On the Charges on the Pore Walls of Microporous Membranes

A. HERNÁNDEZ

DEPARTAMENTO DE FISICA APLICADA II
FACULTAD DE CIENCIAS
UNIVERSIDAD DE VALLADOLID
47071 VALLADOLID, SPAIN

J. A. IBÁÑEZ

DEPARTAMENTO DE FISICA
FACULTAD DE CIENCIAS
UNIVERSIDAD DE MURCIA
30001 MURCIA, SPAIN

L. MARTINEZ-DIEZ and A. F. TEJERINA

DEPARTAMENTO DE FISICA APLICADA II
FACULTAD DE CIENCIAS
UNIVERSIDAD DE VALLADOLID
47071 VALLADOLID, SPAIN



**Abstract**

A method of calculation of the distribution of charges on the pore surfaces of microporous membranes is shown. The membranes are Nuclepore filters separating two diluted NaCl water solutions (concentrations $c_o$ and $c_i > c_o$). The method is based on the integration in the steady state of the Nernst-Planck-Poisson equations by using Goldman's hypothesis of a linear gradient of electric potential. This integration permits us to obtain the volume charge density inside the pores as a function of the distance. In order to obtain the surface density of charges on the pore walls, the pore shape has to be known. It has been proved by us that the pores of our Nuclepore membranes can be described as bent revolution parabolas whose parameters can be determined by adjusting them in order to fit the experimental porosity data. These membranes have very low permselectivities and they are unaffected by the diffusion layers, but the ionic permeabilities are smaller if these diffusion layers exist. This effect on the ionic

permeabilities can be related with the angle of bending and the ratio between mean surface charge densities inside and outside the pores when $c_i = c_o$.

## INTRODUCTION

The use of microporous membranes for the separation of differently sized molecules has recently witnessed increased interest. Industrial applications involve treatment of food and beverage biological materials and waste treatment (*1*). The utility of the process is limited by the inability of the membranes to characterize themselves in relation to the sharpness of separation, so the structure–performance studies are of great interest (*2–6*). The presence of charges inside the pores of microporous membranes are expected to have some influence upon the transport through them, at least when dealing with ionic species (i.e., electrolytic solutions).



Microfiltration and ultrafiltration membranes are frequently characterized by their "molecular weight cut-off," and manufacturers designate an upper limit above which less than 10% transport occurs. This molecular weight cut-off depends on the molecular configuration of the macromolecules, the pore size characteristics of the membrane, and the specific solute adsorption onto the membrane materials (*2*). These adsorption phenomena can take place both on the external surface of the membrane and inside the pores. The small charge carried by some microporous membranes can be of interest even with neutral species. Nevertheless, our studies are well below the molecular weight cut-off in order to avoid any volume exclusion phenomenon. The transport of NaCl–water solutions through Nuclepore membranes with pore radii ranging from 0.1–1.0 μm, as given by the manufacturers, takes place with only the charge-ions interactions playing a role in modifying the free diffusion. This makes it necessary to study these charges inside the pores of Nuclepore membranes whose structure was recently studied by us (*7*).

Membrane potential is one of the most important physical properties of these charge-related membrane processes. Several theories have been proposed in order to explain such membrane potential. One of them is based on the Donnan phase boundary potentials (*8*). Another theory is based on the ion diffusion potential and the Nernst-Planck-Poisson equations (*8*). A combination of these two theories, i.e., the fixed charge membrane theory, which includes the phase boundary potentials (*8*), has been very successful. This membrane potential theory can be improved by using surface potentials, i.e., Gouy-Chapman potentials (*9–12*), instead of phase boundary potentials.

In this paper the volume charge density inside the pores of a passive microporous membrane is studied. A method is explained and applied to several Nuclepore membranes (M02, M04, M06, M10, and M20 with pore diameters of 0.2, 0.4, 0.6, 1.0, and 2.0 μm, which are mean values as given by the manufacturers) separating two dilute NaCl-water solutions with concentrations of $c_o = 100 \times 10^{-7}$ mol/cm$^3$ and $c_i \gg c_o$, of constant temperature: $T = 298.0 \pm 0.1$ K. The Nernst-Planck-Poisson equations can be integrated in the steady state by assuming a linear gradient of electric potential, according to Goldman's hypothesis (*8*). In each membrane-solution interface there is a diffusion boundary layer with a diffusion potential. As a consequence of interactions of ions and water molecules with the solid phase, there is also an electric double layer with a surface potential at each interface.

In order to obtain the surface charge density inside the pores, their structure has to be known. Nuclepore membranes are polycarbonate films perforated by an array of discrete and nearly parallel pores which have been produced by exposure to penetrating radiation followed by activated-track etching. Thermoporometric (*13*) experiments, conductivity, and pure solvent permeability (*3*) experiments and other intrusive methods always give greater mean pore radii than those by nonintrusive methods like scanning electron microscopy (*3, 4, 7*). This is because the chemical treatment creates widenings inside the pores. The shape of the pores of Nuclepore membranes has been experimentally found to be symmetric around its longitudinal axis (*3, 4*), but its shape along the axis has been assumed to have a constant width (cylindrical pores), so-called "spaghetti model" (*5*), or to be linearly increasing in width along the axis (truncated cone pores) (*5*). It has been proved by us (*7*) that the mean pore can be described as obtained by the revolution of a generating parabola around the axis of the pore, with the axis being bent an angle α from the surface of the membrane. This is obtained from experimental and theoretical data of the porosities and is in accordance with transmission microscopy. The parameters of the generating parabola and the angle of bending are experimentally adjustable (*7*).



## THEORY

### Ionic Concentrations and Volume Charge Density

The assumed potential profile is shown in Fig. 1. Note that in each diffusion layer there is a diffusion potential and in each electric double layer there is a Gouy-Chapman potential. Across the membrane itself

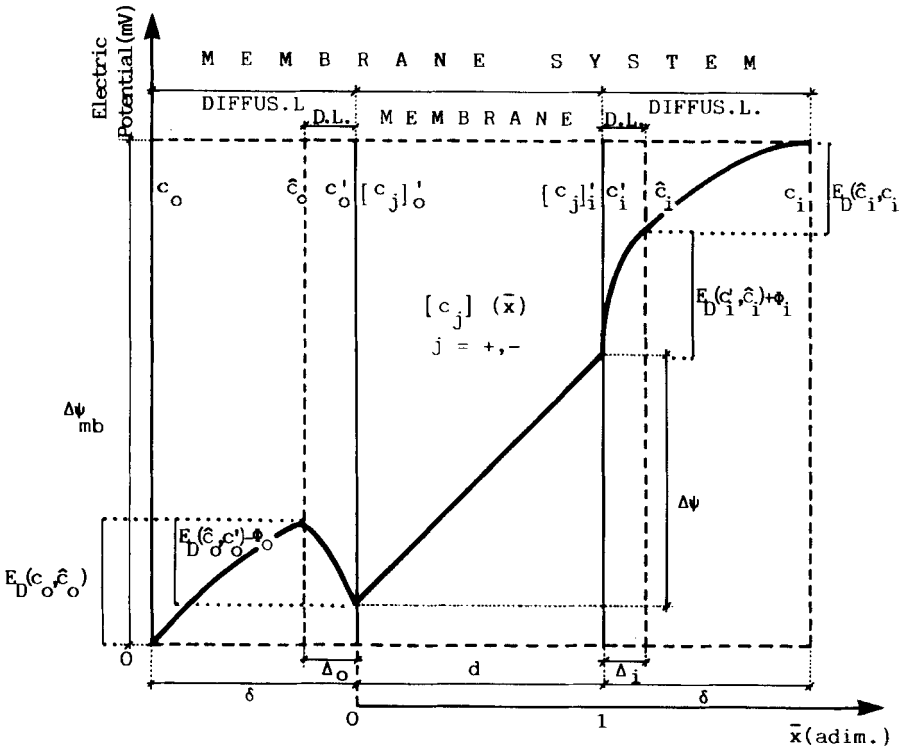


FIG. 1. Profile of electric potential through the membrane system. The membrane potential is $\Delta\psi_{mb}$ and the potential gradient across the membrane is $\Delta\psi/d$. The thickness of both the diffusion layers is $\delta$, the thickness of the membrane is $d$, and those of the electrical double layers are $\Delta_o$ and $\Delta_i$, respectively. The diffusion potential between the solutions of saline concentrations 1 and 2 is $E_D(1,2)$ and $\phi_o$ and $\phi_i$ are the Gouy-Chapman potentials. For the other symbols see the text.

there is a linear potential according to Goldman's hypothesis. The thicknesses of all elements in the membrane system are also shown in Fig. 1. The thicknesses of the two diffusion layers are equal because they come from the same inadequate stirring on both sides of the membrane. The thickness of each double layer, i.e., the Debye length, depends on the concentration of the solution in contact with the membrane.

$c_o$ and $c_i$ denote the concentrations of the bulk solutions ($o$ for the diluted solution and $i$ for the concentrated one). The concentrations at the boundaries of the double layers are $\hat{c}_o$, $c'_o$, $c'_i$, and $\hat{c}_i$. The values of

saline concentrations at the double layer-membrane interfaces (i.e., $c'_o$ and $c'_i$) are obtained from $c_o$ and $c_i$ if we forget the Gouy-Chapman potentials in the electric double layers. So $c'_o$ and $c'_i$ are the concentrations in contact with the membrane if only diffusion acts in the diffusion layers. This is why they are saline concentrations despite there being a separation of ions in the electric double layers; in fact, there is an accumulation of cations on the surfaces of the negatively charged membrane. Therefore the actual concentrations are ionic, $[c_j]'_o$ and $[c_j]'_i$, with j = + for cations and j = − for anions. The volume charge densities at both sides of the membrane are $\bar{\eta}_o$ and $\bar{\eta}_i$. The ionic concentrations in the membrane, $[c_j]$, and the volume charge density inside the pores, $\bar{\eta}$, are space-dependent; i.e., they depend upon the $x$-coordinate whose origin is the membrane-diluted solution contact.

The ionic concentrations $[c_j](x)$ and the volume charge density $\bar{\eta}(x)$ have to be calculated from the other parameters.

The electroneutrality conditions for the membrane boundaries and a 1:1 solute are

$$[c_+]'_p = [c_-]'_p - \bar{\eta}_p \tag{1}$$

with p = 0 for $x = 0$ and p = $i$ for $x = d$. On the other hand, the Donnan balance condition (*10*) leads to

$$[c_+]'_p[c_-]'_p = (c'_p)^2 \tag{2}$$

Using Eqs. (1) and (2), we obtain

$$[c_+]'_p = c'_p - \bar{\eta}_p/2 \tag{3}$$

$$[c_-]'_p = c'_p + \bar{\eta}_p/2 \tag{4}$$

which are valid for $\bar{\eta}_p$ small enough to have $\bar{\eta}_p^2 + 4(c'_p)^2 \simeq 4(c'_p)^2$. Equations (3) and (4) can be joined in

$$[c_j]'_p = c'_p - z_j\bar{\eta}_p/2 \tag{5}$$

where $z_j$ is the valence of the $j$ ion ($z_+ = 1$, $z_- = -1$).

The concentrations $\hat{c}_o$, $c'_o$, $c'_i$, and $\hat{c}_i$ are related to $c_o$ and $c_i$ by

$$c'_o = c_o + J\delta/D_d \tag{6}$$

$$c'_i = c_i - J\delta/D_d \tag{7}$$

$$\hat{c}_o = c'_o - J\Delta_o/D_d \simeq c'_o \tag{8}$$

$$\hat{c}_i = c'_i + J\Delta_i/D_d \simeq c'_i \tag{9}$$

where $J$ is the saline flux and $D_d$ is the saline diffusion coefficient in the diffusion layers. In Eqs. (8) and (9) we have $\delta - \Delta_o \simeq \delta - \Delta_i \simeq \delta$ (*14*).

The permeability of the $j$ ion in the membrane is defined (*8*) as

$$\bar{P}_j = \bar{D}_j/d \tag{10}$$

$\bar{D}_j$ is the $j$-ionic diffusion coefficient in the membrane. The $j$-ionic permeability in the membrane system is

$$P_j = D_j/(d + 2\delta) \tag{11}$$

where $d + 2\delta$ is the $D_j$ thickness. Consequently

$$\bar{P}_j = \gamma P_j \tag{12}$$

$$\gamma = \frac{\bar{D}_j(d + 2\delta)}{D_j d} \tag{13}$$

where $\gamma$ is a constant to be determined below. In writing Eq. (13) it has been assumed that the diffusion and electric double layers do not introduce any new selectivity to the membrane.

In the steady state the scalar Nernst-Planck-Poisson equations with Goldman's hypothesis are (*15*)

$$\frac{J}{\bar{D}_j} = \frac{d[c_j]}{dx} + \frac{z_j F}{RT}\frac{\Delta\psi}{d}[c_j] \tag{14}$$

where $\Delta\psi$ is the electric potential across the membrane. Integration of Eq. (14) leads to

$$[c_j](x) = \beta \exp\left(\frac{-z_j F\Delta\psi}{RTd}x\right) + \frac{JRTd}{\bar{D}_j z_j F\Delta\psi} \tag{15}$$

where $\beta$ is a constant. Using Eq. (5) as boundary conditions for Eq. (15), we get

$$c_i' - z_j \frac{\bar{\eta}_i}{2} = \left( c_o' - z_j \frac{\bar{\eta}_o}{2} - \frac{JRTd}{\bar{D}_j z_j F \Delta\psi} \right) \exp\left( \frac{-z_j F \Delta\psi}{RT} \right) + \frac{JRTd}{\bar{D}_j z_j F \Delta\psi} \tag{16}$$

and using Eq. (10) and $J = P_{SM}(c_i - c_o)$,

$$c_i' - z_j \frac{\bar{\eta}_i}{2} = \left[ c_o' - z_j \frac{\bar{\eta}_o}{2} - \frac{P_{SM}}{\bar{P}_j} \frac{(c_i - c_o)}{z_j} \frac{RT}{F\Delta\psi} \right] \exp\left( -z_j \frac{F\Delta\psi}{RT} \right) + \frac{P_{SM}}{\bar{P}_j} \frac{(c_i - c_o)}{z_j} \frac{RT}{F\Delta\psi} \tag{17}$$

From this equation we obtain

$$[c_j](\bar{x}) = \left[ c_o' - z_j \frac{\bar{\eta}_o}{2} - \frac{P_{SM}}{\bar{P}_j} \frac{(c_i - c_o)}{z_j} \frac{RT}{F\Delta\psi} \right] \exp\left( -z_j \frac{F\Delta\psi}{RT} \bar{x} \right) + \frac{P_{SM}}{\bar{P}_j} \frac{(c_i - c_o)}{z_j} \frac{RT}{F\Delta\psi} \tag{18}$$

where $\bar{x} = x/d$. That is to say:

$$[c_+](\bar{x}) = \left[ c_o' - \frac{\bar{\eta}_o}{2} - \frac{P_{SM}}{\bar{P}_+} \frac{RT}{F\Delta\psi} (c_i - c_o) \right] \exp\left( - \frac{F\Delta\psi}{RT} \bar{x} \right) + \frac{P_{SM}}{\bar{P}_+} \frac{RT}{F\Delta\psi} (c_i - c_o) \tag{19}$$

$$[c_-](\bar{x}) = \left[ c_o' + \frac{\bar{\eta}_o}{2} + \frac{P_{SM}}{\bar{P}_-} \frac{RT}{F\Delta\psi} (c_i - c_o) \right] \exp\left( + \frac{F\Delta\psi}{RT} \bar{x} \right) - \frac{P_{SM}}{\bar{P}_-} \frac{RT}{F\Delta\psi} (c_i - c_o) \tag{20}$$

From Eq. (17) we obtain

$$\Delta\psi = \frac{RT}{F} P_{SM}(c_i - c_o) \left\{ \left[ \frac{1}{\bar{P}_+} - \frac{1}{\bar{P}_-} \right] \frac{1}{c_o + c_i} + \frac{\bar{\eta}_o - \bar{\eta}_i}{2[(c_o')^2 - (c_i')^2]} \left[ \frac{1}{\bar{P}_+} + \frac{1}{\bar{P}_-} \right] \right\} \tag{21}$$

where we have made the approximation

$$(c_i'^2 - c_o'^2) + \frac{\bar{\eta}_o^2 - \bar{\eta}_i^2}{4} \simeq c_i'^2 - c_o'^2$$

If we call the expression given in Eq. (21) $\Delta\Phi$, but with $P_j$ instead of $\bar{P}_j$, we have

$$\Delta\psi = \Delta\Phi/\gamma \tag{22}$$

then using Eqs. (12), (17), and (22) we calculate $\gamma$ as

$$\gamma = \frac{F\Delta\Phi}{RT}\left[\ln\left(\frac{c_i' + \frac{\bar{\eta}_i}{2} P_{SM}(c_i - c_o)RT/F\Delta\Phi P_-}{c_o' + \frac{\bar{\eta}_o}{2} P_{SM}(c_i - c_o)RT/F\Delta\Phi P_-}\right)\right]^{-1} \tag{23}$$

then from Eqs. (6), (7), (12), (21), and (23) we can calculate $\bar{P}_j$ from $P_j$, $c_o$, $c_i$, $\bar{\eta}_o$, $\bar{\eta}_i$, $P_{SM}$, and $\delta/D_d$.

The electroneutrality condition requires that, inside the membrane,

$$\bar{\eta}(\bar{x}) = [c_-](\bar{x}) - [c_+](\bar{x}) \tag{24}$$

From Eqs. (19), (20), and (24) it follows that

$$\bar{\eta}(\bar{x}) = \left[c_o' + \frac{\bar{\eta}_o}{2} + \frac{P_{SM}}{\bar{P}_-}\frac{RT}{F\Delta\psi}(c_i - c_o)\right]\exp\left(\frac{F\Delta\psi}{RT}\bar{x}\right)$$

$$- \left[c_o' - \frac{\bar{\eta}_o}{2} - \frac{P_{SM}}{\bar{P}_+}\frac{RT}{F\Delta\psi}(c_i - c_o)\right]\exp\left(-\frac{F\Delta\psi}{RT}\bar{x}\right)$$

$$- P_{SM}\frac{RT}{F\Delta\psi}(c_i - c_o)\left(\frac{1}{\bar{P}_+} + \frac{1}{\bar{P}_-}\right) \tag{25}$$

Then we can calculate $\bar{\eta}(\bar{x})$ from $P_+$, $P_-$, $c_o$, $c_i$, $\bar{\eta}_o$, $\bar{\eta}_i$, $P_{SM}$, and $\delta/D_d$. Because we have yet to calculated $\bar{P}_+$ and $\bar{P}_-$, $c_o'$ and $c_i'$ can be calculated from Eqs. (6) and (7) and $\Delta\psi$ from Eq. (21).

We wish to emphasize the following points:

(a) The ratio $\delta/D_d$ was previously calculated (*16*)
(b) The permeability of the membrane system $P_{SM}$ was obtained in one

experiment from measurements of saline fluxes ($P_{SM} = J/(c_i - c_o)$) (*16*)

(c) The ionic permeabilities $P_-$ and $P_+$ of the membrane system were obtained by combining the measurements of ion fluxes and membrane potentials (*15*)

(d) The volume densities of charges in the membrane interphases, $\bar{\eta}_o$ and $\bar{\eta}_i$, can be calculated for each $c_o$ and $c_i$, taking into account the diffusion boundary layers from the respective values of the surface charge densities $\bar{\sigma}_o$ and $\bar{\sigma}_i$ (*14*)

In Table 1 we show the values of $\delta/D_d$, $P_{SM}$, $P_-$, and $P_+$ for the microporous Nuclepore membranes M02, M04, M06, M10, and M20 bathed by two NaCl solutions stirred at 50 rpm at 298.0 ± 0.1 K.



## Pore Shape and Surface Charge Density

The surface charge density, $\bar{\sigma}(\bar{x})$, is

$$\bar{\sigma}(\bar{x}) = \frac{V_p}{S_p}(\bar{x})\bar{\eta}(\bar{x}) \tag{26}$$

where $V_p$ and $S_p$ are the volume and surface of the mean pore, respectively. It is evident that in general $V_p/S_p$ depend upon $\bar{x}$. For cylindrical pores we have

$$V_p/S_p = r/2 \tag{27}$$

where $r$ is the mean pore radius.

We proved (*7*) that the mean pore of a Nuclepore membrane, at least

TABLE 1
Permeability Parameters of the Nuclepore Filters Studied

| Membranes | $\delta/D_d$ (s/cm) | $P_{SM} \times 10^4$ (cm/s) | $P_- \times 10^4$ (cm/s) | $P_+ \times 10^4$ (cm/s) |
|---|---|---|---|---|
| M02 | 255 ± 20 | 4.5 ± 0.3 | 6.5 ± 0.3 | 3.4 ± 0.1 |
| M04 | 255 ± 20 | 4.0 ± 0.3 | 5.8 ± 0.3 | 3.0 ± 0.1 |
| M06 | 255 ± 20 | 4.8 ± 0.2 | 6.5 ± 0.3 | 3.8 ± 0.1 |
| M10 | 255 ± 20 | 4.4 ± 0.2 | 5.3 ± 0.2 | 3.8 ± 0.1 |
| M20 | 255 ± 20 | 5.9 ± 0.3 | 8.3 ± 0.4 | 4.5 ± 0.2 |

for M02-M20, can be described as bent at an angle α between it and the membrane surface and with an internal maximal radius $r_i$ at the center of the membrane. A mean pore is shown in Fig. 2. Obviously α and $r_i$ are different for each Nuclepore filter. In Table 2 are shown α, $r$, and $r_i$. The mean external radius of the pores, $r$, has been measured from SEM (scanning electron microscopy).

If for each $x$ we substitute the revolution paraboloid by a tangential cylinder, we have

$$\frac{V_p}{S_p}(\bar{x}) = \frac{r(\bar{x})}{2} \tag{28}$$

where $r(\bar{x})$ is the equation of the generating bent parabola, which is

$$r(x) = -4\frac{r_i - r}{(d/\sin\alpha)^2}\left(\frac{x}{\sin\alpha}\right)^2 + 4\frac{r_i - r}{d/\sin\alpha}\left(\frac{x}{\sin\alpha}\right) + r \tag{29}$$

Therefore $\bar{\sigma}(\bar{x})$ can be obtained from Eqs. (25), (26), (28), and (29). The mean surface density inside the membrane is

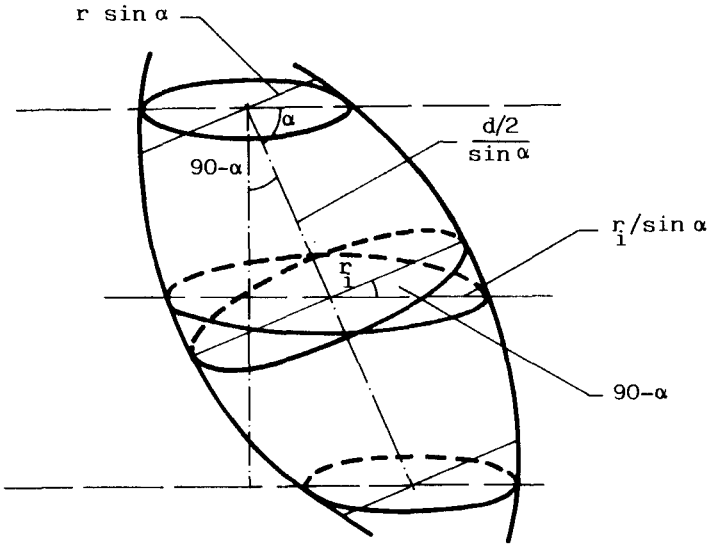


FIG. 2. A mean pore bent an angle α with respect to the membrane surface. The pore radii are very much smaller and the thickness of the membrane, $d$, is very much greater than drawn. Therefore, the generating parabola is much flatter than in the drawing.

TABLE 2
Mean Structural Parameters of the Nuclepore Filters Studied

| Membranes | α (degrees) | $r$ (μm) | $r_i$ (μm) |
|---|---|---|---|
| M02 | 25 ± 1 | 0.060 ± 0.001 | 0.14 ± 0.01 |
| M04 | 32 ± 1 | 0.190 ± 0.003 | 0.30 ± 0.02 |
| M06 | 24 ± 1 | 0.217 ± 0.004 | 0.41 ± 0.02 |
| M10 | 24 ± 1 | 0.411 ± 0.008 | 0.95 ± 0.04 |
| M20 | 17 ± 1 | 0.780 ± 0.009 | 0.97 ± 0.04 |

$$\langle \bar{\sigma} \rangle = \frac{\int_0^1 \bar{\sigma}(\bar{x}) 2\pi r(\bar{x}) d\bar{x}}{\int_0^1 2\pi r(\bar{x}) d\bar{x}} \tag{30}$$

but using Eqs. (26) and (28):

$$\langle \bar{\sigma} \rangle = \frac{\int_0^1 \bar{\eta}(\bar{x}) \frac{r^2(\bar{x})}{2} d\bar{x}}{\int_0^1 r(\bar{x}) d\bar{x}} \tag{31}$$

Therefore, from Eqs. (25), (29), and (31) we obtain

$$\begin{aligned}\langle \bar{\sigma} \rangle = &\left[ c_o' + \frac{\bar{\eta}_o}{2} + \frac{P_{SM}}{\bar{P}_-} \frac{RT}{F\Delta\psi} (c_i - c_o) \right] \\ &\times (W_1 P_1 + W_2 P_2 + W_3 P_3 + W_4 P_4 + W_5 P_5) \\ &- \left[ c_o' - \frac{\bar{\eta}_o}{2} - \frac{P_{SM}}{\bar{P}_-} \frac{RT}{F\Delta\psi} (c_i - c_o) \right] \\ &\times (W_1 Q_1 + W_2 Q_2 + W_3 Q_3 + W_4 Q_4 + W_5 Q_5) \\ &- P_{SM} \frac{RT}{F\Delta\psi} (c_i - c_o) \left( \frac{1}{\bar{P}_+} + \frac{1}{\bar{P}_-} \right) \left( \frac{W_1}{5} + \frac{W_2}{4} + \frac{W_3}{3} + \frac{W_4}{2} + W_5 \right)\end{aligned} \tag{32}$$

where

$$P_1 = \frac{e^G}{G}\left(1 - \frac{4}{G} + \frac{12}{G^2} - \frac{24}{G^3} + \frac{24}{G^4}\right) - \frac{24}{G^5}$$

$$P_2 = \frac{e^G}{G}\left(1 - \frac{3}{G} + \frac{6}{G^2} - \frac{6}{G^3}\right) + \frac{6}{G^4}$$

$$P_3 = \frac{e^G}{G}\left(1 - \frac{2}{G} + \frac{2}{G^2}\right) - \frac{2}{G^3}$$

$$P_4 = \frac{e^G}{G}\left(1 - \frac{1}{G}\right) + \frac{1}{G^2}$$

$$P_5 = \frac{e^G}{G} - \frac{1}{G}$$

$$Q_1 = \frac{e^{-G}}{-G}\left(1 + \frac{4}{G} + \frac{12}{G^2} + \frac{24}{G^3} + \frac{24}{G^4}\right) + \frac{24}{G^5}$$

$$Q_2 = \frac{e^{-G}}{-G}\left(1 + \frac{3}{G} + \frac{6}{G^2} + \frac{6}{G^3}\right) + \frac{6}{G^4}$$

$$Q_3 = \frac{e^{-G}}{-G}\left(1 + \frac{2}{G} + \frac{2}{G^2}\right) + \frac{2}{G^3}$$

$$Q_4 = \frac{e^{-G}}{-G}\left(1 + \frac{1}{G}\right) + \frac{1}{G^2}$$

$$Q_5 = \frac{e^{-G}}{-G} + \frac{1}{G}$$

$$G = F\Delta\psi/RT$$

$$W_1 = 16(r_i - r)^2 \Big/ \left(\frac{11}{6}r - \frac{5}{6}r_i\right)2$$

$$W_2 = -32(r_i - r)^2 \Big/ \left(\frac{11}{6}r - \frac{5}{6}r_i\right)2$$

$$W_3 = 8[2(r_i - r)^2 - (r_i - r)r] \Big/ \left(\frac{11}{6}r - \frac{5}{6}r_i\right)2$$

$$W_4 = 8(r_i - r)r \Big/ \left(\frac{11}{6}r - \frac{5}{6}r_i\right)2$$

$$W_5 = r^2 \Big/ \left(\frac{11}{6}r - \frac{5}{6}r_i\right)2$$

Therefore we can calculate $\langle\bar{\sigma}\rangle$ for each $c_o$ and $c_i$ by using Eq. (32). Note that the angle of bending of a mean pore is not explicitly needed in order to calculate $\langle\bar{\sigma}\rangle$. Nevertheless, the mean internal radius, $r_i$, is characteristic of a bent pore; i.e., if we assume a nonbent pore, we would obtain another value for $r_i$. The volume charge densities $\bar{\eta}_o$ and $\bar{\eta}_i$ can be calculated from $\bar{\sigma}_o$ and $\bar{\sigma}_i$ (*14*) by using Eqs. (26) and (27).

## RESULTS AND DISCUSSION

In Table 3 the anionic and cationic permeabilities through the M02–M20 membranes are shown. The permselectivities (i.e., the ratio between anionic and cationic permeabilities) that we have assumed to be equal for each membrane and the corresponding membrane system are also shown. Note that the permselectivities are very low and very close to each other. The values of $\gamma$ are also shown in Table 3. The value of $\gamma$ gives an idea of the decrease of ionic fluxes due to the presence of diffusion layers. They are very close to but greater than 1; i.e., it would be desirable to avoid diffusion layers but the increase ionic fluxes obtained would be very small.

In Fig. 3 the electric potential through the membrane, $\Delta\psi$, is plotted versus the relative saline concentration, $n_c = c_i/c_o$. These potentials are not linear with $\ln c_i/c_o$, which was the case with the membrane potential,

TABLE 3
Calculated Ionic Permeabilities, Permselectivities, and Relations between Ionic Permeabilities of the Membranes and of the Membrane Systems, $\gamma$

| Membranes | $\bar{P}_- \times 10^4$ (cm/s) | $\bar{P}_+ \times 10^4$ (cm/s) | Permselectivity, $\bar{P}_-/\bar{P}_+ = P_-/P_+$ (adimensional) | $\gamma$, $\bar{P}_-/P_- = \bar{P}_+/P_+$ (adimensional) |
|---|---|---|---|---|
| M02 | 8.33 ± 0.02 | 4.36 ± 0.01 | 1.91 ± 0.01 | 1.28 ± 0.01 |
| M04 | 7.23 ± 0.02 | 3.74 ± 0.01 | 1.93 ± 0.01 | 1.25 ± 0.01 |
| M06 | 8.52 ± 0.02 | 4.98 ± 0.01 | 1.71 ± 0.01 | 1.31 ± 0.01 |
| M10 | 6.76 ± 0.02 | 4.85 ± 0.01 | 1.39 ± 0.01 | 1.28 ± 0.01 |
| M20 | 11.88 ± 0.02 | 6.44 ± 0.02 | 1.85 ± 0.01 | 1.43 ± 0.01 |

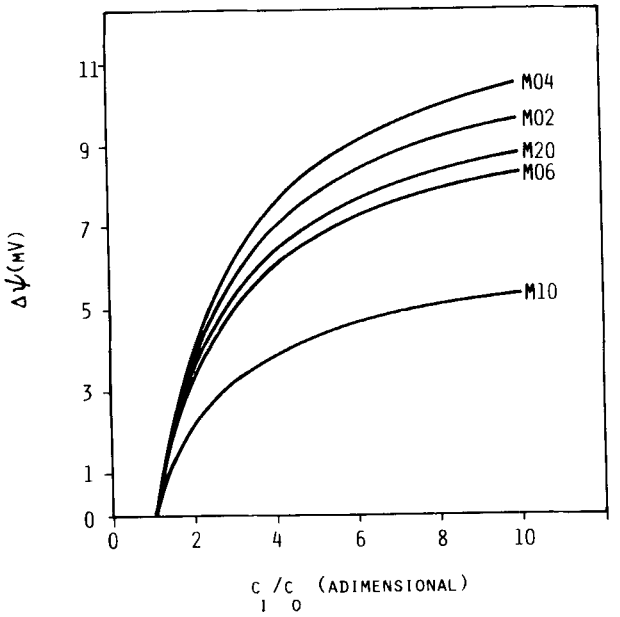


FIG. 3. The electric potential through the membrane itself versus the relative saline concentration $c_i/c_o$ for the Nuclepore filters studied.



$\Delta\psi_{mb}$ (*15*), at least for $c_o = 100 \times 10^{-7}$ mol/cm$^3$, and $100 \times 10^{-7}$ mol/cm$^3 \leqslant c_i \leqslant 1000 \times 10^{-7}$ mol/cm$^3$.

In Fig. 4 we see the natural logarithm of the anionic permeability of the membrane itself, ln $\bar{P}_-$, as a function of the anionic permeability of the membrane system, $P_-$. From this figure and the adjusted curve we conclude that, for our membranes, solutions, stirring speed, and temperature (actually these two last parameters are not relevant in determining the basic shape of the curve), $\bar{P}_-$ increases with $P$ as an exponential ($\bar{P}_- = (2.42 \pm 0.29) \exp [(0.191 \pm 0.017)P_-]$).

In Figs. 5 and 6 we show the surface charge density inside a mean pore in absolute value $-\bar{\sigma}$ as a function of the adimensionalized distance, $\bar{x}$, for the membranes M02 and M20, respectively. Note that the charges are low but there is an accumulation on the walls of the center of the pores. This accumulation is in general higher for bent pores than for nonbent ones.

In Fig. 7 the mean surface charge density in absolute value $-\langle\bar{\sigma}\rangle$ is plotted versus the relative saline concentration $n_c = c_i/c_o$. The curves cross each other for some values of $n_c$. Nevertheless, the significant surface

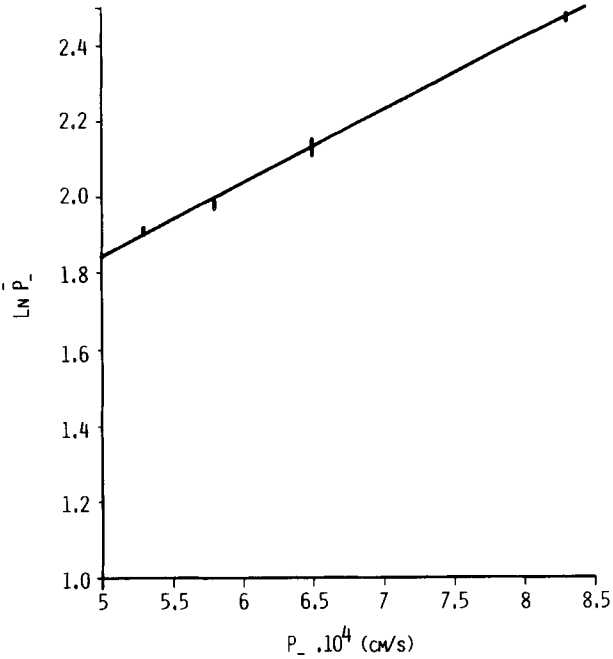


FIG. 4. The natural logarithm of the anionic permeability of the membrane itself, ln $\bar{P}_-$, versus the anionic permeability of the membrane system, $P_-$. The fitted curve is $\ln \bar{P}_- = (0.885 \pm 0.120) + (0.191 \pm 0.017)P_-$.

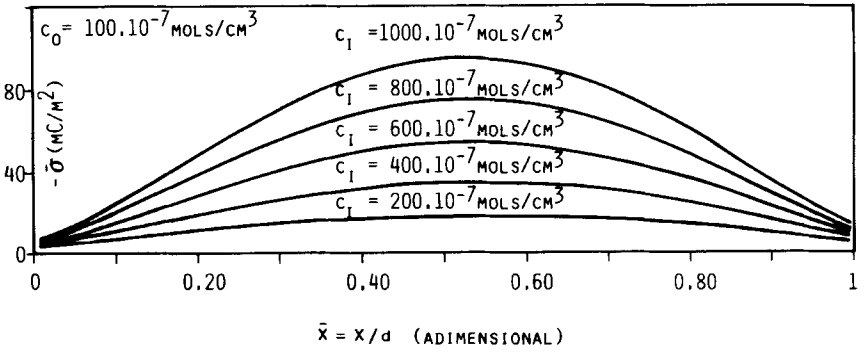


FIG. 5. Surface charge density inside a mean pore in absolute value as a function of the adimensionalized distance, $-\bar{\sigma}(\bar{x})$, for the membrane M02.

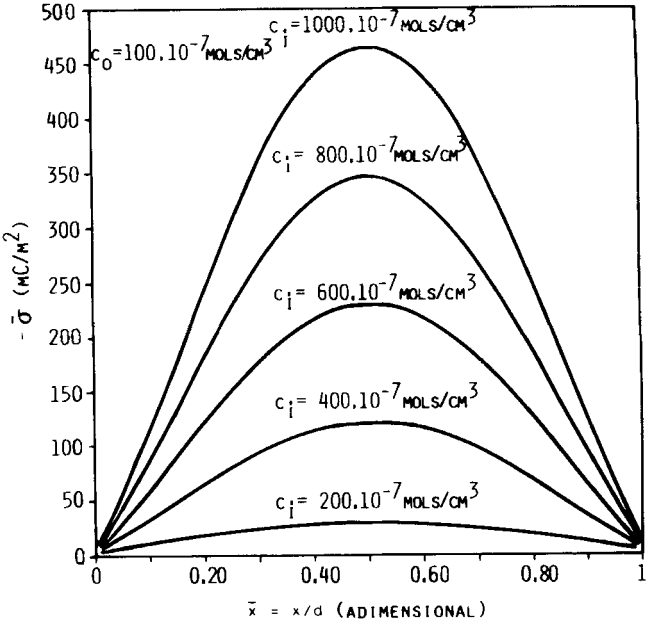


FIG. 6. Surface charge density inside a mean pore in absolute value as a function of the adimensionalized distance, $-\bar{\sigma}(\bar{x})$, for the membrane M20.



charge densities (*14*) are those for $c_i = c_o$, so in Table 4 the mean surface charge density inside the pores, $\langle\bar{\sigma}\rangle$ (from extrapolation in Fig. 7), and on the external surfaces, $\bar{\sigma}_s$ (*14*), when $n_c \to 1$ are shown with the ratio between them. This ratio gives an idea about the degree of overcharge inside the pores compared with the external surfaces.

In Fig. 8 the ratio $\bar{P}_-/P_-$ is plotted as a function of $\langle\bar{\sigma}\rangle/\bar{\sigma}s$ when $n_c \to 1$. The adjusted curve is a parabola ($y = (1.827 \pm 0.190) - (0.457 \pm 0.219)x + (0.091 \pm 0.061)x^2$ with $y = \bar{P}_-/P_-$ and $x = \lim_{n_c \to 1}(\langle\bar{\sigma}\rangle/\bar{\sigma}s)$). Note that when $(\langle\bar{\sigma}\rangle/\bar{\sigma}s)_{n_c \to 1}$ increases, $\bar{P}_-/P_-$ decreases; i.e., when the overcharge of the pores is great, the importance of the diffusion layers as barriers to ionic transport is small. This is foreseeable because then the membrane is the most important barrier in the membrane system.

In Fig. 9, $\gamma = P_-/P_-$ is shown as a function of the bending angle $\alpha$. The adjusted curve is $\gamma = (2.140 \pm 0.378) - (0.058 \pm 0.031)\alpha + (0.0009 \pm 0.0006)\alpha^2$. Note that for bending angles greater than approximately 32°, the sign of the slope of the curve changes; i.e., the importance of the diffusion layers as barriers to ionic transport increases with $\alpha$ but only for

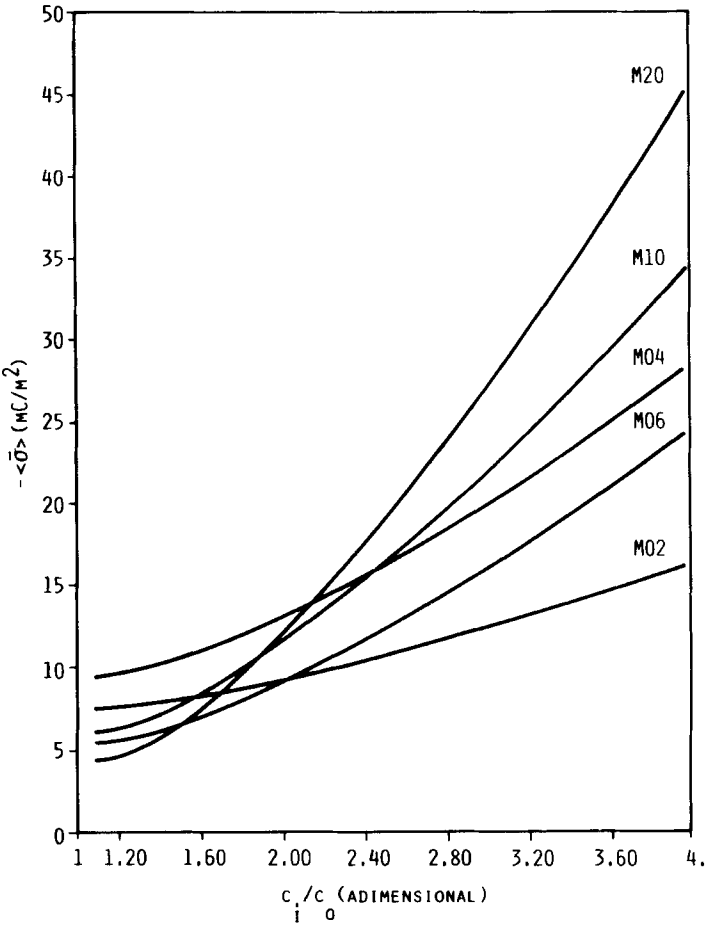


FIG. 7. The mean surface charge density in absolute value, $-\langle\bar{\sigma}\rangle$, inside the pores of the Nuclepore filters studied as a function of the relative saline concentration $c_i/c_o$.

TABLE 4
Calculated Mean Surface Charge Densities on the Pore Walls, Surface Charge Densities on the External Surfaces of the Membranes, and the Ratio $\langle\bar{\sigma}\rangle/\bar{\sigma}_s$ ($c_i = c_o$)

| Membranes | $-\langle\bar{\sigma}\rangle(n_c\to 1)$ (mC/m$^2$) | $-\bar{\sigma}_s(n_c\to 1)$ (mC/m$^2$) | $\langle\bar{\sigma}\rangle(n_c\to 1)/\bar{\sigma}_s(n_c\to 1)$ (adimensional) |
|---|---|---|---|
| M02 | 8.05 ± 0.01 | 4.03 ± 0.01 | 2.998 ± 0.01 |
| M04 | 10.68 ± 0.02 | 4.28 ± 0.01 | 2.495 ± 0.01 |
| M06 | 5.95 ± 0.01 | 3.61 ± 0.01 | 1.650 ± 0.01 |
| M10 | 6.47 ± 0.01 | 3.11 ± 0.01 | 2.080 ± 0.01 |
| M20 | 4.47 ± 0.01 | 3.97 ± 0.01 | 1.130 ± 0.01 |

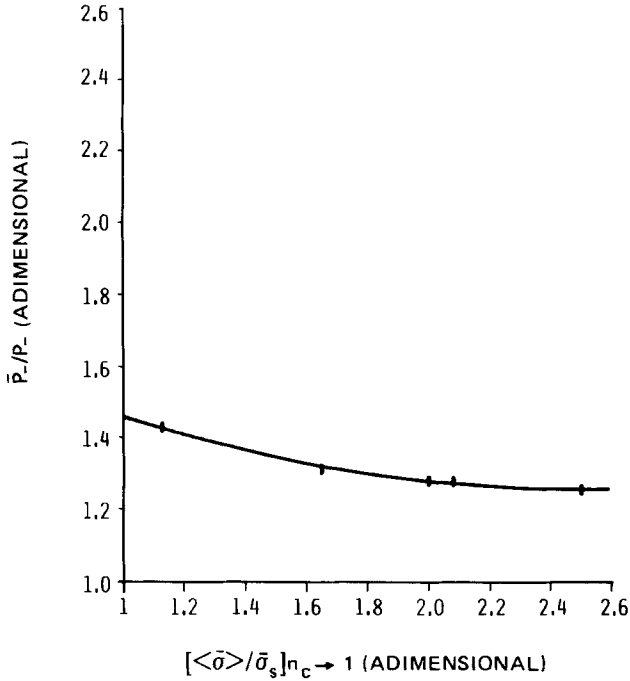


FIG. 8. The ratio $\bar{P}_-/P_-$ as a function of $\langle\bar{\sigma}\rangle/\bar{\sigma}_s$ when $c_i = c_o$ (i.e., when $n_c \equiv c_i/c_o \to 1$). If we call $x \equiv \lim_{n_c \to 1} (\langle\bar{\sigma}\rangle/\bar{\sigma}_s)$ and $y \equiv \bar{P}_-/P_-$, the fitted curve is $y = (1.827 \pm 0.190) - (0.457 \pm 0.219)x + (0.091 \pm 0.061)x^2$.



very bent pores ($\alpha$ small), while for slightly bent pores ($\alpha$ large) it decreases with $\alpha$. This is because pores with a mean bending angle of $\alpha \simeq 0°$ or $\alpha \simeq 90°$ have a very small membrane barrier.

## REFERENCES

1. G. Belfort, *Synthetic Membrane Processes, Fundamentals and Water Applications,* Academic, New York, 1984.
2. M. Bodzek, "Physico-Chemical Characterization of Ultrafiltration Membranes," *Pol. J. Chem., 57,* 919 (1983).
3. G. Guillot, L. Léger, and F. Rondelez, "Diffusion of Large Flexible Polymer Chains through Model Porous Membranes," *Macromolecules, 18,* 2531 (1985).
4. S. Manabe, Y. Shigemoto, and K. Kamide, "Determination of Pore Radius Distribution of Porous Polymeric Membranes by Electron Microscopic Method," *Polym. J., 17*(6), 775 (1985).
5. M. Nishimura and Y. Mizutani, "Correlation between Structure and Properties of

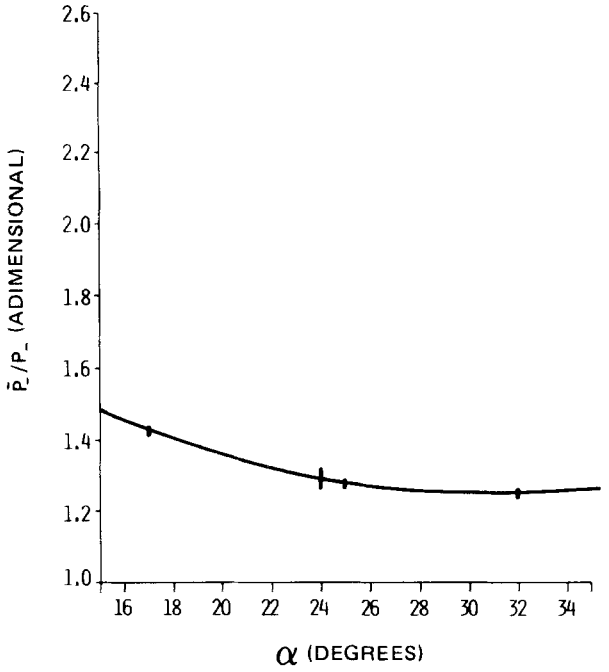


FIG. 9. The ratio $\bar{P}_-/P_-$ as a function of the bending angle $\alpha$. The fitted curve is $\bar{P}_-/P_- = (2.140 \pm 0.378) - (0.058 \pm 0.031)\alpha + (0.0009 \pm 0.0006)\alpha^2$.



Cation-Exchange Membranes Prepared by the Paste Method," *J. Appl. Electrochem., 11,* 165 (1981).

6. A. Tanioka, K. Ishikawa, A. Kakuta, M. Kuramoto, and M. Ohno, "Pore Size Evaluation for Fine Porous Freeze Dried Cellulose Acetate Membrane by Gas Separation," *J. Appl. Polym. Sci., 30,* 695 (1985).
7. A. Hernández, F. Martínez-Villa, J. A. Ibáñez, J. I. Arribas, and A. F. Tejerina, "An Experimentally Fitted and Simple Model for the Pores in Nuclepore Membranes," *Sep. Sci. Technol., 21*(6&7), 665 (1986).
8. N. Laksminarayanayah, *Equations of Membrane Biophysics,* Academic, New York, 1984.
9. S. Ohki, "Membrane Potential Surface Potential and Ionic Permeability," *Phys. Lett., 75A,* 149 (1979).
10. M. J. Sparnaay, *The Electrical Double Layer,* Pergamon, Oxford, 1972.
11. J. O'M. Bockris and A. K. Reddy, *Modern Electrochemistry. An Introduction to an Interdisciplinary Area,* Plenum, New York, 1975.
12. E. Gileadi, E. Kirowa-Eisner, and J. Penciner, *Interfacial Electrochemistry. An Experimental Approach,* Addison-Wesley, Reading, Massachusetts, 1975.
13. C. Eyraud, "Thermoporometry," in *Communications of the 1st Summer School on Membrane Science and Technology,* Cadarache, France, September 3-7, 1984.

*14.* A. Hernández, J. A. Ibáñez, and A. F. Tejerina, "True and Adsorbed Charges in Passive Membranes Surface. Charge Density and Ionic Selectivity of Several Microporous Membranes," *Sep. Sci. Technol., 20*(4), 297 (1985).
*15.* J. A. Ibáñez, A. Hernández, and A. F. Tejerina, "Determination of Ionic Permeabilities from Passive Membrane Potentials," *J. Non-Equilib. Thermodyn., 7,* 159 (1982).
*16.* J. A. Ibáñez, A. F. Tejerina, J. Garrido, and J. Pellicer, "Intrinsical Characteristics of Passive Membranes from Membrane System Permeability, Pore Radius and Pore Density," *Ibid., 5,* 379 (1980).

*Received by editor July 11, 1986*